The Astrophysical Journal, 732:94 (10pp), 2011 May 10 doi:10.1088/0004-637X/732/2/94
© 2011. The American Astronomical Society. All rights reserved. Printed in the U.S.A.

EARLY-TYPE GALAXIES AT $z \sim 1.3$. III. ON THE DEPENDENCE OF FORMATION EPOCHS AND STAR FORMATION HISTORIES ON STELLAR MASS AND ENVIRONMENT

A. Rettura[1,2,3], S. Mei[4,5], S. A. Stanford[1,6], A. Raichoor[5], S. Moran[2], B. Holden[7], P. Rosati[8], R. Ellis[9], F. Nakata[10], M. Nonino[11], T. Treu[12], J. P. Blakeslee[13], R. Demarco[14], P. Eisenhardt[15], H. C. Ford[4], R. A. E. Fosbury[8], G. Illingworth[7], M. Huertas-Company[4,5], M. J. Jee[1], T. Kodama[16], M. Postman[17], M. Tanaka[18], and R. L. White[17]

[1] Department of Physics, University of California, Davis, CA 95616, USA
[2] Department of Physics and Astronomy, Johns Hopkins University, Baltimore, MD 21218, USA
[3] Department of Physics and Astronomy, University of California, Riverside, CA 92521, USA
[4] University of Paris Denis Diderot, 75205 Paris Cedex 13, France
[5] GEPI, Observatoire de Paris, Section de Meudon, Meudon Cedex, France
[6] Institute of Geophysics and Planetary Physics, Lawrence Livermore National Laboratory, Livermore, CA 94551, USA
[7] UCO/Lick Observatories, University of California, Santa Cruz, CA 92065, USA
[8] European Southern Observatory, 85748 Garching, Germany
[9] California Institute of Technology, Pasadena, CA 91125, USA
[10] Subaru Telescope, National Astronomical Observatory of Japan, Hilo, HI 96720, USA
[11] INAF-Osservatorio Astronomico di Trieste, 34131 Trieste, Italy
[12] Department of Physics, University of California, Santa Barbara, CA 93106, USA
[13] Herzberg Institute of Astrophysics, National Research Council of Canada, Victoria, BC V9E 2E7, Canada
[14] Department of Astronomy, Universidad de Concepcion, Casilla 160-C, Concepcion, Chile
[15] Jet Propulsion Laboratory, California Institute of Technology, MS 169-327, Pasadena, CA 91109, USA
[16] National Astronomical Observatory of Japan, Mitaka, Tokyo 181-8588, Japan
[17] Space Telescope Science Institute, Baltimore, MD 21218, USA
[18] Institute for the Physics and Mathematics of the Universe, The University of Tokyo, 5-1-5 Kashiwanoha, Kashiwa-shi, Chiba 277-8583, Japan
Received 2010 November 22; accepted 2011 March 4; published 2011 April 21

ABSTRACT

We study the environmental dependence of stellar population properties at $z \sim 1.3$. We derive galaxy properties (stellar masses, ages, and star formation histories) for samples of massive, red, passive early-type galaxies (ETGs) in two high-redshift clusters, RXJ0849+4452 and RXJ0848+4453 (with redshifts of $z = 1.26$ and 1.27, respectively), and compare them with those measured for the RDCS1252.9−2927 cluster at $z = 1.24$ and with those measured for a similarly mass-selected sample of field contemporaries drawn from the GOODS-South field. Robust estimates of the aforementioned parameters have been obtained by comparing a large grid of composite stellar population models with extensive 8- to 10-band photometric coverage, from the rest-frame far-ultraviolet to the infrared. We find no variations of the overall stellar population properties among the different samples of cluster ETGs. However, when comparing cluster versus field stellar population properties we find that, even if the ages are similar and depend only on galaxy mass, the ones in the field do employ longer timescales to assemble their final mass. We find that, approximately 1 Gyr after the onset of star formation, the majority (75%) of cluster galaxies have already assembled most (>80%) of their final mass, while, by the same time, fewer (35%) field ETGs have. Thus, we conclude that while galaxy mass regulates the timing of galaxy formation, the environment regulates the timescale of their star formation histories.

Key words: cosmology: observations – galaxies: clusters: general – galaxies: elliptical and lenticular, cD – galaxies: evolution – galaxies: formation – galaxies: star formation

Online-only material: color figures

1. INTRODUCTION

Galaxies reside in environments that span a wide range of density. In order to understand the physical processes that drive their evolution it is important to test for systematic differences between galaxies in various environments. Many authors have shown that population density plays an important role in determining many galaxy properties, such as star formation rate (SFR), gas content, and morphology (Kodama & Bower 2001; Balogh et al. 2002). Several mechanisms have been proposed by theorists to account for these effects, such as ram pressure stripping, mergers, and tidal effects (Gunn & Gott 1972; Dressler et al. 1997; Moore et al. 1996, 1998, 1999).

More than half of all stars in the local universe are found in massive spheroids (e.g., Bell et al. 2003). The history of mass assembly and star formation (SF) of these early-type galaxies (ETGs) are among the most actively pursued elements in galaxy evolution studies, and form the basis for models of massive galaxy formation (Renzini 2006).

Galaxy clusters provide an ideal laboratory to study ETGs, the dominant galaxy population in clusters, even beyond redshift one. In addition, large field surveys have multiplied in recent years, extending the baseline over which environmental effects can be studied.

Studies indicate that the most massive ETGs in the field may be amongst the oldest at any given epoch (Cimatti et al. 2004; Fontana et al. 2004; Saracco et al. 2004; Treu et al. 2005; Juneau et al. 2005; di Serego Alighieri et al. 2005; Pannella et al. 2009). They have evolved mainly passively since $z \sim 1$ and, at least the most massive ones, as slowly as cluster galaxies (van Dokkum & Franx 1996, 2001; Bernardi et al. 1998; Treu et al. 1999, 2001; Kochanek et al. 2000; van Dokkum & Stanford 2003; De Propris et al. 2007). Similarly, tight constraints have been placed on the scatter and slope of the color–magnitude relation

Table 1
Cluster and Field Photometric Data Sets

Filter	Lynx E (Telescope/Instrument)	Lynx W (Telescope/Instrument)	CL1252 (Telescope/Instrument)	CDFS (Telescope/Instrument)
u'	Keck/LRIS	Keck/LRIS	VLT/VIMOS (U)	VLT/VIMOS (U)
B	...	...	VLT/FORS2	*HST*/ACS/F435W
V	...	...	VLT/FORS2	*HST*/ACS/F606W
R	Keck/LRIS	Keck/LRIS	VLT/FORS2	...
i_{F775W}	*HST*/ACS	*HST*/ACS	*HST*/ACS	*HST*/ACS
z_{F850LP}	*HST*/ACS	*HST*/ACS	*HST*/ACS	*HST*/ACS
J	KPNO/FLAMINGOS	KPNO/FLAMINGOS	VLT/ISAAC (J_s)	VLT/ISAAC
Ks	KPNO/FLAMINGOS	KPNO/FLAMINGOS	VLT/ISAAC	VLT/ISAAC
[3.6 μm]	*Spitzer*/IRAC	*Spitzer*/IRAC	*Spitzer*/IRAC	*Spitzer*/IRAC
[4.5 μm]	*Spitzer*/IRAC	*Spitzer*/IRAC	*Spitzer*/IRAC	*Spitzer*/IRAC

(CMR), the fundamental plane (FP; Jørgensen et al. 2006; Treu et al. 2005; van der Wel et al. 2005; di Serego Alighieri et al. 2006; van Dokkum & van der Marel 2007), and Balmer line strengths (Clemens et al. 2006; Sánchez-Blázquez et al. 2006) of the ETGs populating massive clusters, indicating a very high formation redshift for the ETGs in clusters as well (Rettura et al. 2006, 2010; Eisenhardt et al. 2008; Gobat et al. 2008; Mei et al. 2009; Collins et al. 2009; Rosati et al. 2009).

The most distant clusters known to date provide the strongest leverage on model predictions (Papovich et al. 2010; Tanaka et al. 2010b). Specifically, there is a tight CMR of ETGs at $0.8 < z < 1.5$ (Blakeslee et al. 2003, 2006; Mei et al. 2006a, 2006b; Lidman et al. 2008; Hilton et al. 2009; Strazzullo et al. 2010), a slowly evolving K-band luminosity function seemingly at odds with hierarchical merging scenarios (Toft et al. 2004; Strazzullo et al. 2006), and a tight and slowly evolving FP out to $z \approx 1.2$ (Holden et al. 2005). The existence of such massive, passively evolving galaxies already at $z \gtrsim 0.8$ needs to be reconciled with the evidence for massive (often dusty) star-forming populations found at $z \gtrsim 2.2$ both in the field and in overdense environments (Steidel et al. 2005; Adelberger et al. 2005; Kodama et al. 2007; Miley & De Breuck 2008; Overzier et al. 2009; Tanaka et al. 2010a).

Previous studies based on optical and infrared data have placed some constraints on the star formation histories (SFHs) of ETGs in distant clusters based on the scatter in their CMRs: the best-fit models yield formation epochs of $2 < z_f < 7$ (Blakeslee et al. 2003), but a greater accuracy could not be achieved based on the available rest-frame optical and infrared data alone. The reason for this is that age-dependent features in galaxy spectra (e.g., the 4000 Å break or the 1.6 μm bump) are too broad or evolve too slowly to be used as adequate age indicators (Burstein et al. 1988; Tantalo et al. 1996; Maraston 2005; Rettura et al. 2010). In order to better constrain the formation epoch (z_f) of ETGs, we need to probe the much sharper and fast-evolving rest-frame UV-optical colors that will allow us to determine z_f with much greater accuracy than hitherto achieved, enabling us to better constrain the entire SFH of ETGs[18] (see also Figure 2 of Rettura et al. 2010).

In order to provide a key test of the paradigm of an accelerated evolution in the highest density environments (Diaferio et al. 2001; Thomas et al. 2005), in this work, on the basis of photometric data available over the rest-frame wavelength range 0.15–2 μm, we compare stellar masses, ages and inferred SFHs of ETGs found in three massive X-ray detected clusters at $z \sim 1.3$ (RXJ0849+4452, RXJ0848+4453, and RDCS1252.9−2927) with a sample of field contemporaries drawn from the GOODS-South field.

The structure of this paper is as follows. The description of our data sets, cataloging and sample selection is given in Section 2. In Section 3, we describe our methods in inferring SFHs, ages, and masses from stellar population analysis. The results of our study are discussed in Section 4, while in Section 5, we summarize our conclusions.

We assume a $\Omega_\Lambda = 0.73$, $\Omega_m = 0.27$, and $H_0 = 71$ km s^{-1} Mpc^{-1} flat universe (Spergel et al. 2003), and use magnitudes in the AB system throughout this work.

2. DESCRIPTION OF THE DATA

This work is based on data collection programs on the three galaxy clusters at $z \sim 1.3$ which are amongst the most extensive spectroscopic and photometric surveys available over the wavelength range 0.35–4.5 μm. To compare cluster galaxy properties with the field, we also take advantage of similar-quality archival data available for the GOODS-South field. Table 1 summarizes the rich and homogeneous data set employed in this study.

2.1. RX J0849+4452 and RX J0848+4453

The Lynx Supercluster is the highest redshift supercluster known today (Nakata et al. 2005), with two central X-ray detected galaxy clusters and three spectroscopically confirmed surrounding groups. This work focuses in particular on the cores of the two main clusters, RX J0849+4452 (hereafter Lynx E) and RX J0848+4453 (hereafter Lynx W), both detected in the *ROSAT* Deep Cluster Survey (Rosati et al. 1999) and spectroscopically confirmed at $z = 1.261$ (Rosati et al. 1999) and $z = 1.273$ (Stanford et al. 1997), respectively. Furthermore, in two accompanying papers (Raichoor et al. 2011; Mei et al. 2011), we also compare ETGs' stellar population properties in the two cluster cores with those of the ones in the surrounding groups.

Both Lynx E and Lynx W were observed in the u' filter with the blue channel of LRIS on Keck I in two separate epochs. On 2003 March 4, exposures totaling 260 minutes were obtained in conditions that were photometric with 0.″8 seeing. A further 240 minutes were obtained during the night of 2008 March 1, with clear skies and a typical seeing of 0.″9. The two epochs of data were reduced separately using standard IRAF tasks, where we subtracted the bias level, flat-fielded each exposure using a series of twilight flats obtained on each night, astrometrically calibrated and aligned each image

[18] Note that by $z \gtrsim 1.3$ not enough cosmic time has elapsed for horizontal-branch stars to produce the "UV upturn" (Yi et al. 1997, 1999).

by comparison to star positions from the *HST* GSC2.2 catalog and then refined with a larger number of stellar positions from the Sloan Digital Sky Survey DR6 catalog. Finally, the images were flux calibrated, also correcting for atmospheric extinction, using exposures of various photometric standard stars obtained across a range of air masses each night, and then combined. The two sets of images were taken at different position angles, and so the combined frame has an effective exposure time of 8 hr and 20 minutes across much of the field, but a shallower depth at the edges of the field where the frames do not overlap. The effective resolution in the combined ultraviolet image is 0.″95.

In order to sample the optical-to-infrared wavelength domain, we have obtained data in the following passbands: R, i_{F775W}, z_{F850LP}, J, Ks, and *Spitzer*/IRAC channels, 3.6 μm (ch1) and 4.5 μm (ch2).

We refer the reader to the companion paper by Raichoor et al. (2011) for a more detailed description of the optical and infrared data set used in this work (see also their Table 1).

Here, we recall that the R-band images were obtained with the Keck/LRIS instrument. The i_{F775W} and z_{F850LP} bands were observed in the $F775W$ and $F850LP$ filters provided by the Advanced Camera for Surveys (ACS) wide field camera on board the *Hubble Space Telescope* (*HST*). We note that these two observing filters have been purposely chosen to bracket the 4000 Å break of a model elliptical galaxy at $z = 1.26$–1.27 (Mei et al. 2006a, 2006b).

The near-infrared imaging data (J, K_s bands) were acquired with the FLAMINGOS instrument available at the Kitt Peak National Observatory (KPNO).

Mid-infrared imaging was obtained (in two channels at [3.6 μm] and [4.5 μm]) with the IRAC camera on board the *Spitzer Space Telescope*.

2.2. RDCS1252.9−2927 and the GOODS-South Field

This work builds on data sets and analyses already performed on ETGs belonging to the X-ray luminous cluster, RDCS1252.9−2927 (hereafter CL1252), and to the GOODS-South field, centered on the so-called Chandra Deep Field South field (hereafter CDFS), as reported by Rettura et al. (2010) and Gobat et al. (2008).

We refer to the aforementioned papers for more details on the data reduction. Here, we note that the data we have employed for the CL1252 cluster consist of deep imaging in 10 bands: Very Large Telescope (VLT)/VIMOS (U), VLT/FORS2 (B, V, R), *HST*/ACS (i_{F775W}, z_{F850lp}) (Blakeslee et al. 2003), VLT/ISAAC (J_s, K_s) (Lidman et al. 2004), *Spitzer*/IRAC (3.6 μm, 4.5 μm), as well as spectroscopic data taken with VLT/FORS2 and published in Demarco et al. (2007).

The archival data for the comparison field, the CDFS, comprise deep imaging in nine bands: VLT/VIMOS (U) (Nonino et al. 2009), *HST*/ACS (B_{F435W}, V_{F606W}, i_{775W}, z_{F850LP}) (Giavalisco et al. 2004), VLT/ISAAC, (J, K_s) (Retzlaff et al. 2010), *Spitzer*/IRAC (3.6 μm, 4.5 μm),[19] as well as spectroscopic data taken with the VLT/FORS2 300I grism by the ESO-GOODS survey[20] (Vanzella et al. 2005, 2006, 2008; Balestra et al. 2010) and the K20 survey (Cimatti et al. 2002).

[19] CDFS imaging is publicly available through the GOODS collaboration Web site: http://www.stsci.edu/science/goods/.

[20] Spectroscopic data are publicly available through the Web site: http://www.eso.org/sci/activities/projects/goods/MasterSpectroscopy.htm.

2.3. Cataloging of Observations and Samples Selection

The resulting data sets for the three clusters and the field have homogeneous depths and wavelength coverage, allowing the application of similar selection criteria for both samples. This is a crucial point for stellar population studies, so that we do not have different levels of systematic biases in the analyses.

The data allow the reconstruction of galaxy spectral energy distributions (SEDs) by entirely sampling the relevant spectrum range emitted by all the different stellar populations. For each observing band we produce catalogs from matched aperture photometry, with an aperture of radius 1.″5 and an aperture correction out to 7″ radius, as described in Rettura et al. (2006) and Raichoor et al. (2011).

The availability of 8–10 passbands spanning such a large wavelength range enables the estimate of accurate stellar masses (Rettura et al. 2006), ages and SFHs of ETGs (Rettura et al. 2010) and enables us to directly compare galaxy properties of homogeneously selected samples of ETGs in both environments.

Specifically, we measure stellar population parameters of Lynx E and Lynx W early-type cluster galaxies and compare them with those found for similarly selected samples of cluster and field contemporaries drawn from CL1252 at $z = 1.237$ and CDFS at $z = 1.237 \pm 0.15$.

We estimated stellar masses from both K_s band observations and SED fitting. The two estimates give similar mass limits. The depth of the VLT/ISAAC and KPNO/FLAMINGOS K_s-band images and the extended multi-wavelength data for all fields allow us, in fact, to define complete mass-selected samples. The reader is referred to Gobat et al. (2008) and Raichoor et al. (2011) for more details. Here, we note that overall photometric completeness is obtained if we limit our analysis to stellar masses larger than $M_{\rm lim} = 5 \times 10^{10}\ M_{\odot}$.[21]

A selection of Lynx E, Lynx W, and CL1252 passive ETGs along the cluster red sequence is efficiently provided by a color selection of $i_{F775W} - z_{F850LP} > 0.8$ (Blakeslee et al. 2003; Mei et al. 2006a, 2006b, 2009, 2011).

For CL1252, in the spectroscopic sample of Demarco et al. (2007), there are 22 red-sequence galaxies ($i_{F775W} - z_{F850LP} > 0.8$) with $M_* > M_{\rm lim}$, of which 18 are classified as passive ETGs, i.e., without detectable [O II] or other emission lines in their observed spectra. For Lynx E and Lynx W, in the combined photometric and spectroscopic samples (Mei et al. 2006a; Stanford et al. 1997, 2001; Rosati et al. 1999; van Dokkum & Stanford 2003; B. Holden et al. 2011, private communication), there are 21 red-sequence galaxies with $M_* > M_{\rm lim}$, of which 17 are classified as passive ETGs. Specifically, there are 10 passive spectroscopically confirmed ETGs in Lynx E, and 3 in Lynx W. We remark that, to improve the statistics, we have also included in the Lynx ETG sample three photometrically confirmed members of Lynx E and one photometrically confirmed member of Lynx W both with $i_{F775W} - z_{F850LP} > 0.8$ and $M_* > M_{\rm lim}$, thus resulting in a total sample of 17 Lynx E+W ETGs. It is important to note that the removal from our sample of these four galaxies, whose cluster membership was assessed on the basis of an (8- to 9-band) photometric redshift only, would not change the main conclusions of this study.

[21] Assuming Salpeter Initial Mass Function (IMF), with lower and upper cutoffs, $m_L = 0.1\ M_{\odot}$ and $m_U = 100\ M_{\odot}$, respectively. We refer the reader to Rettura et al. (2006) and Raichoor et al. (2011) for a discussion on the dependence of inferred stellar population properties on the actual choice of the IMF.

For the corresponding CDFS sample of field contemporaries, the same criteria yield 27 passive ETGs in CDFS with FORS2 spectra giving redshift in the range $z = 1.237 \pm 0.15$ (for more details see also Gobat et al. 2008 and Rettura et al. 2010).

We also remark that, adopting the classification scheme of Postman et al. (2005), visual morphological analysis of the *HST*/ACS images available for all samples indicates that all our red, passive ETGs also show typical elliptical or lenticular morphology.

As reported in Rettura et al. (2010), we also recall that the spectroscopic follow-up for CL1252 is more complete at the low-mass end than in CDFS. Thus, our sample of ETGs in CDFS is likely to be more incomplete at the low-mass end than the CL1252 and Lynx ones. We will return to this point when discussing our results in Section 4.

3. DATA ANALYSIS: DERIVATION OF STELLAR POPULATION PROPERTIES

The data described in the previous section are used to infer the fundamental physical properties of similarly mass-selected samples of early-type galaxies (13 ETGs in the Lynx E, 4 in Lynx W, 18 in CL1252, and 27 in the CDFS). Adopting a similar approach to Rettura et al. (2006, 2010), we derive stellar masses, SFHs and ages for each ETG in Lynx E and Lynx W using multi-wavelength point-spread-function-matched aperture photometry from eight passbands, from observed u' band to observed 4.5 μm. For each galaxy, we compare the observed SED with a set of composite stellar populations (hereafter CSP) templates computed with the Bruzual & Charlot (2003) models, assuming solar metallicity, Salpeter (1955) IMF and no dust.

Similarly to Rettura et al. (2006), we checked the effect of dust extinction on the best-fit stellar masses by including a fourth free parameter, $0.0 < E(B-V) < 0.4$, following the Cardelli et al. (1989) prescription. Performing the SED fit on 13 Lynx E+W ETGs (all with complete u'-to-4.5 μm coverage) and on 22 CDFS ETGs (all with complete U-to-4.5 μm coverage), we find that in ~50% of the cases $E(B-V) \leqslant 0.05$ gives the best fit. In the remaining cases values of $E(B-V) \leqslant 0.2$ are found and no particular trend with mass nor environment is found either, hence supporting the validity of the dust-free assumption we make throughout this work.

For our CSP models, we assume the following grid of exponentially declining SFH scenarios, $\Psi(t, \tau)$:

$$\Psi(t, \tau) = \mathrm{SFR}_0 \cdot e^{-t/\tau} \left[\frac{M_\odot}{\mathrm{yr}} \right], \quad (1)$$

where $0.05\,\mathrm{Gyr} \leqslant \tau \leqslant 5\,\mathrm{Gyr}$, SFR_0 is the initial SFR at the onset of SF, and t is the time since the onset of SF[22] of the stellar population model formed at a look-back time $T(\overline{z}) + t$, with, e.g., $T \simeq 8.67$ Gyr at the epoch of observation ($\overline{z} \simeq 1.3$).

In determining galaxy model ages, masses and SFHs from SED fitting, it is important to understand how much our estimates could possibly be affected by "age-metallicity"[23] and "age-SFH" degeneracies. We note that in Rettura et al. (2010), we have demonstrated that the use of photometric information coming from the rest-frame UV is crucial to distinguish the different parameters of the stellar population modeling, allowing us to break the "age-SFH degeneracy." It is also important to note that the rest-frame UV remains also largely unaffected by the "age-metallicity" degeneracy, which plagues optical studies (Worthey 1994).

Furthermore, the reliability, at $z > 1$, of stellar population parameters inferred in the rest-frame NIR regime ($\lambda_{\mathrm{obs}} \sim 2\,\mu$m) has long been debated (Maraston 1998) because of the different implementation of the relevant short-duration thermally pulsating asymptotic giant branch phase in the different stellar population synthesis models. However, in Rettura et al. (2006) we have shown that different stellar population models actually yield overall consistent stellar masses, within the typical errors, for ETGs at $z \sim 1.0$. It is clear that the inferred SFH (and age) is model-dependent and is generally not a unique solution; however, the relative difference in the underlying stellar population is still significant. In fact, in Rettura et al. (2010) we have shown that when comparing *cluster* versus *field* τs and ages, the *relative* differences among samples (or lack thereof, as in their Figure 8) were similar regardless of the actual stellar population code used, not affecting their conclusions.

Hence, since our study is indeed aimed at constraining the relative difference of galaxy stellar population parameters in a *cluster* versus *cluster* and *cluster* versus *field* fashion, we will only show here the results obtained with the Bruzual & Charlot (2003) models, in order to facilitate direct comparison with previous studies in the literature. Note that in Raichoor et al. (2011) we also present an extensive discussion on systematics due to choice of the stellar population models at $z \sim 1.3$.

To account for the average age of the bulk of the stars in a galaxy, we refer throughout this paper to SF *weighted* ages, $\langle t \rangle_{\mathrm{SFH}}$, defined as

$$\langle t \rangle_{\mathrm{SFH}} \equiv \frac{\int_0^t (t - t') \Psi(t', \tau)\, dt'}{\int_0^t \Psi(t', \tau)\, dt'}. \quad (2)$$

Assuming $\Psi(t', \tau)$ as in Equation (1) we obtain

$$\langle t \rangle_{\mathrm{SFH}} = \frac{t - \tau + \tau \cdot e^{-\frac{t}{\tau}}}{1 - e^{-\frac{t}{\tau}}}, \quad (3)$$

where t is the time elapsed since the onset of SF.

By comparing each observed SED with these atlases of synthetic spectra, we construct a three-dimensional χ^2 space spanning a wide range of SFHs, model ages and stellar masses. The galaxy mass in stars M_*, the inferred $\langle t \rangle_{\mathrm{SFH}}$ and the τ of the models giving the lowest χ^2 are taken as the best-fit estimates of the galaxy stellar mass, age, and SFH timescale throughout this work. We note that this procedure results in typical errors for galaxy ages of ~0.5 Gyr, and for τ of ~0.2 Gyr (Rettura et al. 2010). Typical uncertainties on the mass determination are about ~40% (i.e., 0.15 dex; Rettura et al. 2006).

4. RESULTS AND DISCUSSION

In the top panel of Figure 1, we plot the inferred stellar masses as a function of the $U-B$ rest-frame color for the mass-selected samples of CL1252, Lynx E and Lynx W ETGs, resulting in a very similar distribution. In the bottom panel of Figure 1 we show the rest-frame $U-B$ color–mass diagram of the combined samples of cluster (red circles) and field (blue circles) ETGs. To have a very simple estimate of the scatter of the color–mass relation, as derived from the SED fitting, we derive the scatter

[22] The range of acceptable ts for a given galaxy has been limited by the age of the universe at its observed redshift.

[23] We employ the working assumption that the most-massive ETGs have all solar metallicities.

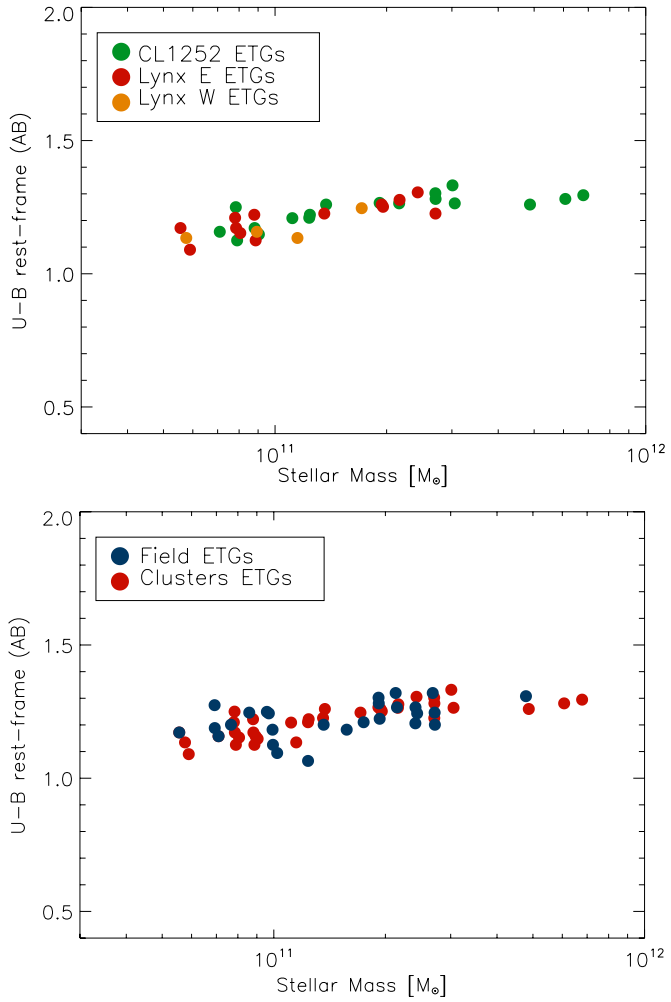

Figure 1. Top panel: rest-frame $U-B$ color–mass diagram of mass-selected samples of CL1252 (green circles), Lynx E (red circles), and Lynx W (orange circles) passive cluster ETGs. Uncertainties in the stellar mass are ∼0.15 dex. Bottom panel: $U-B$ color–mass diagram of the combined samples of Cluster (red circles) and Field (blue circles) ETGs. Field ETGs galaxies are distributed around the cluster red sequence, although they are found with a larger scatter.

(A color version of this figure is available in the online journal.)

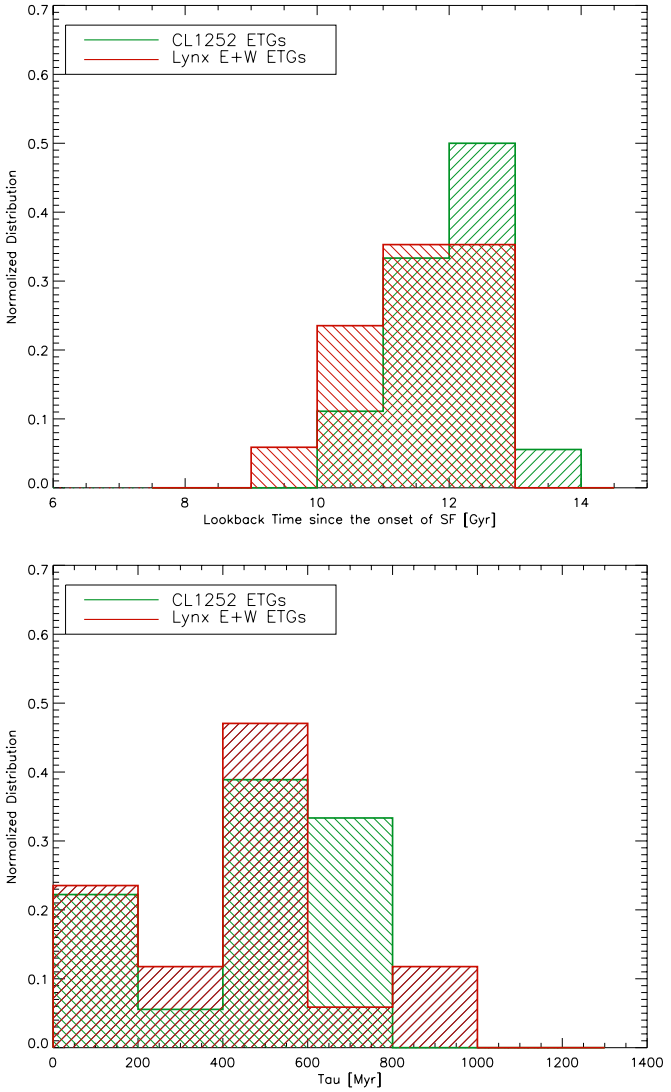

Figure 2. Top panel: histograms of the look-back times to the onsets of SF for the cluster samples. Uncertainties in ages are ∼0.5 Gyr. No cluster-to-cluster variation of the galaxy ages is found. Bottom panel: formation timescales, τ, histograms for the different cluster samples. No cluster-to-cluster variation of the galaxy formation timescales is found. Uncertainties in stellar masses and τ are ∼0.15 dex and ∼0.2 Gyr, respectively.

(A color version of this figure is available in the online journal.)

around the fit using a Tukey's biweight (Press et al. 1992). We simply calculated the uncertainty in the scatter estimation by bootstrapping on 1000 simulations. For the Lynx cluster sample, CL1252, and field galaxies, we obtain a scatter of 0.031 ± 0.010, 0.042 ± 0.010, and 0.050 ± 0.008, respectively. These are intrinsic scatters as predicted from the best SED fitting, and do not take into account uncertainties in the fitting methods. Field ETGs galaxies are distributed around the cluster red sequence, although they seem to show a larger scatter, especially at lower masses. We will need more statistics and better estimates of uncertainties to draw a stringent conclusion, since the cluster and field overall scatters could still be consistent within the uncertainties.

As we apply the method described in Section 3, we are able to directly compare the relative distribution of galaxy stellar population properties for the different samples. Stellar masses ranges from $M_{\rm lim}$ to $4 \times 10^{11}\ M_{\odot}$ except for three CL1252 bright galaxies and one galaxy in the field (bottom panel of Figure 1). We do not find any of the Lynx clusters ETGs to be more massive than $3 \times 10^{11}\ M_{\odot}$ (top panel of Figure 1).

We want to test the hypothesis that two samples' stellar-mass distributions have the same median against the hypothesis that they differ at the 5% significance level. The Mann–Whitney U-test suggests that the distributions are likely to be similar (median probability of 44%). We also study the Kolmogorov–Smirnov (K-S) statistic and associated probability that the two arrays of data are drawn from the same distribution, yielding a similar result. A high value (67%) of probability shows that the cumulative distribution function of the cluster stellar masses is not significantly different from the field one.

As shown in Figure 2, we also find that all clusters show the same relative distributions of look-back time since the onset of SF ($T(\overline{z})+t$, top panel) and stellar mass assembly timescales (τ, bottom panel). In fact, both the Mann–Whitney U-test (median probability of 10%, 21%) and the K-S statistics (75%, 91% of probability) also elucidate that the distributions are very similar.

This lack of cluster-to-cluster variation may well indicate that these three clusters experienced similar evolutionary processes, resulting in similar stellar population properties shown by their member ETGs. Since these samples of cluster ETGs are found

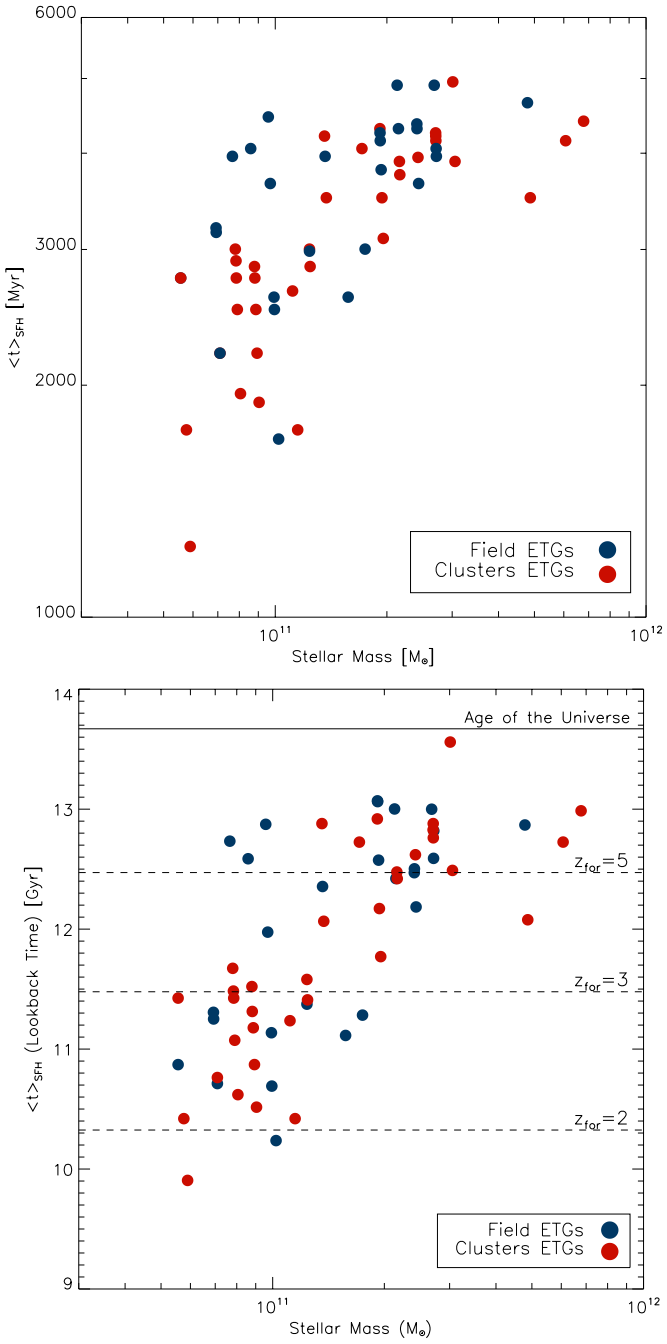

Figure 3. Top panel: the dependence of the SF weighted ages on the galaxy mass and environment. No dependence of ages on the environment is found. Bottom panel: the dependence of the look-back time to SF weighted ages on the galaxy mass and environment. Uncertainties in stellar masses and ages are ∼0.15 dex and ∼0.5 Gyr.

(A color version of this figure is available in the online journal.)

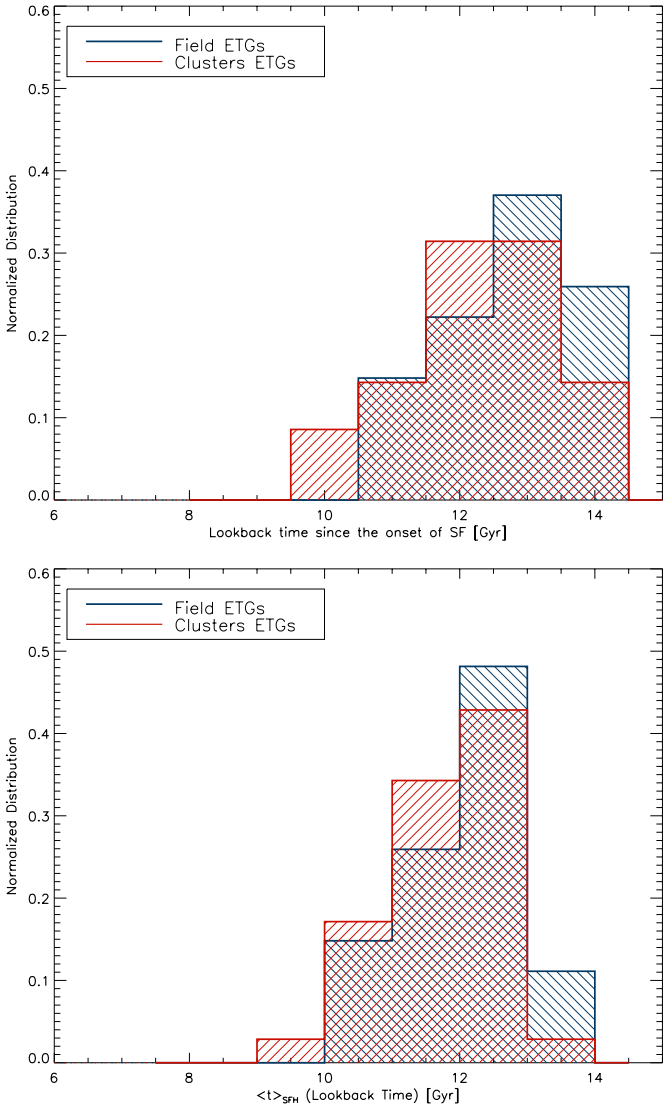

Figure 4. Histograms of the field (solid blue line) and cluster (solid red line) look-back times since the onset of SF (top panel) and of the SF weighted ages (bottom panel). There is no dependence of the ETG ages on the environment. Uncertainties in age determination are ∼0.5 Gyr.

(A color version of this figure is available in the online journal.)

to be very similar from a stellar population point of view, we can combine them into one sample of 35 ETGs, representative of the Cluster environment at $z \sim 1.3$, apt for comparison with the sample of 27 CDFS ETGs, representative of the Field environment.

Thus, we compare the distribution of the SF weighted ages ($\langle t \rangle_{\rm SFH}$, top panel of Figure 3) as a function of the stellar mass in both environments. We find the distributions to be overall very similar, as also shown by the histograms of look-back times since the onset of SF (top panel of Figure 4) and by the histograms of the look-back times to $\langle t \rangle_{\rm SFH}$ (bottom panel of Figure 4). Note that the Mann–Whitney *U*-test returns a median probability of 18% and the K-S statistics a 60% probability that the last two data values are drawn from the same distribution. These results imply that no significant delay in relative age is found for ETGs in either environment. Using BC03 models, we find that ∼80% of ETGs have SF weighted ages in the range 3.5 ± 1.0 Gyr in both cluster and field, in qualitative agreement with previous CMR studies (Blakeslee et al. 2003; Mei et al. 2006a, 2006b).

In the bottom panel of Figure 3 we show, for both samples, the dependence of SF weighted ages, $\langle t \rangle_{\rm SFH}$, on stellar mass. It is evident that the ages of ETGs only depend on their masses, i.e., the halo mass in which they reside, which is in agreement with the so-called *downsizing* scenario of galaxy formation (Cowie et al. 1996). We note that this scenario has also been reconciled with the introduction of various forms of so-called feedback mechanisms, with the recent versions of semi-analytic models based on ΛCDM cosmogony (De Lucia et al. 2006; Bower et al. 2006; Menci et al. 2008).

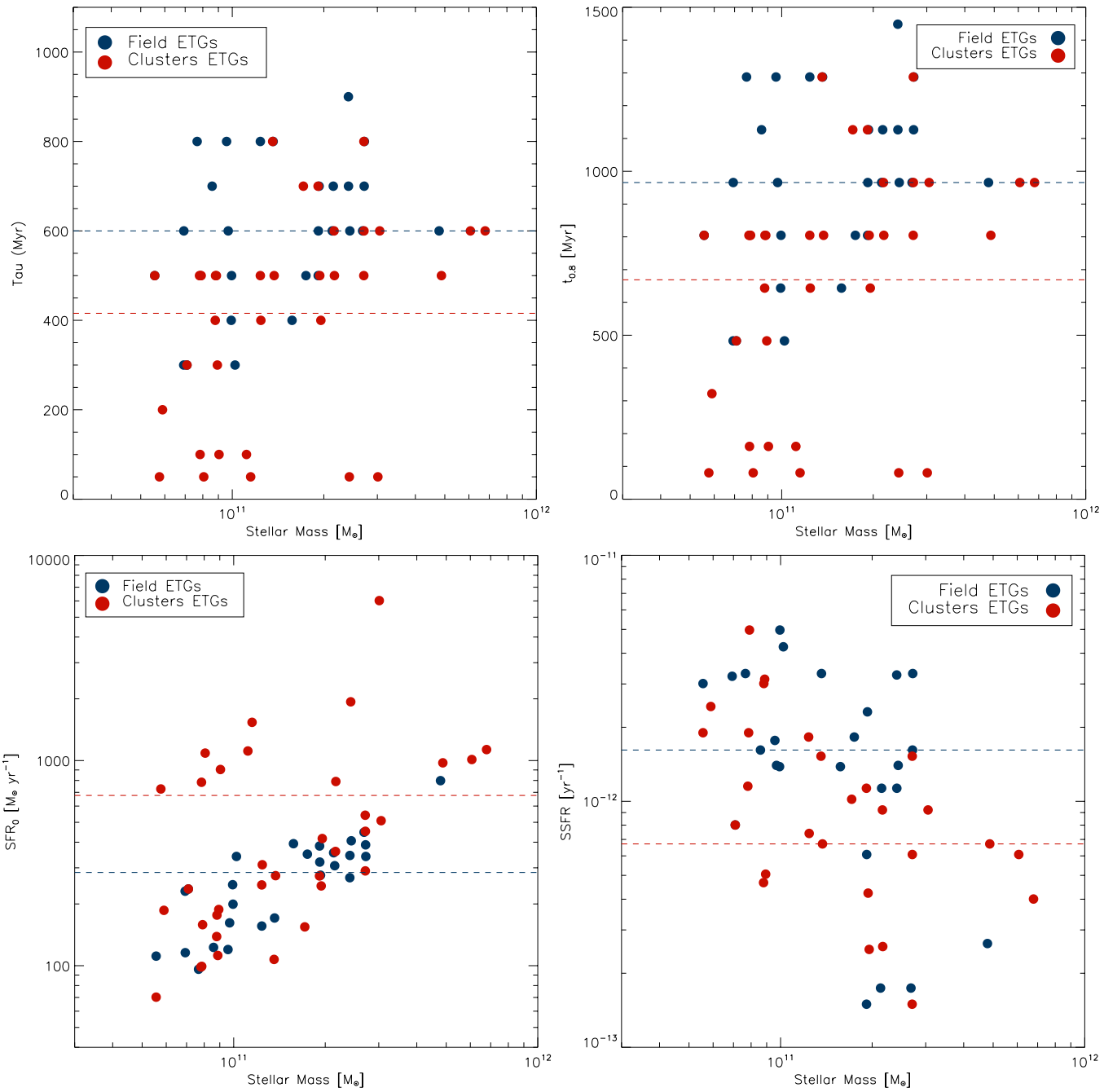

Figure 5. Top left panel: formation timescales, τ, of ETG as a function of their stellar mass and environment. Top right panel: as a function of stellar mass and environment, the diagram of the time, $t_{0.8}$, needed for a given galaxy to form 80% of the stars it will have at $z = 0$. Bottom left panel: dependence of the initial SFR, SFR_0, of ETGs on their stellar mass and environment. Bottom right panel: specific SFRs, SSFR, of ETGs as a function of their stellar mass and environment. The mean error in stellar age is 0.5 Gyr. Uncertainties in stellar masses, τ, and $t_{0.8}$, are ∼0.15 dex, ∼0.2, and ∼0.4 Gyr, respectively. In all panels, as a function of stellar mass, the median values of the different cluster (red dashed line) and field (blue dashed line) stellar population parameter distributions are also indicated.

(A color version of this figure is available in the online journal.)

To summarize, we find that cluster galaxy (SF weighted) ages have the same relative distribution as their field contemporaries: no significant delay in their formation epochs is found within the errors (∼0.5 Gyr). We recall that this result is in remarkably good agreement with the ones derived by van Dokkum & van der Marel (2007) and di Serego Alighieri et al. (2006) from the evolution of the mass-to-light ratio (M/L). However, our method is able to extend this kind of analysis to a less massive system than the typical targets of FP studies at $z \sim 1$.

Despite the fact that cluster and field galaxy formation epochs are found to be similar, it could still be possible that the timescales of their SFHs are significantly different. As mentioned above, the data have shown that the distributions of cluster and field optical colors were slightly different. As a function of the stellar mass, cluster galaxies are found to lie on a very tight red sequence, while those in the field populate the same color sequence with a slightly larger scatter (Figure 1).

This piece of evidence finds a natural explanation in the framework of our modeling. As shown in the top left panel of Figure 5, as a function of stellar mass, we find that field ETGs show longer SFH timescales than their cluster contemporaries, which tend to assemble their mass with the shortest τ at any

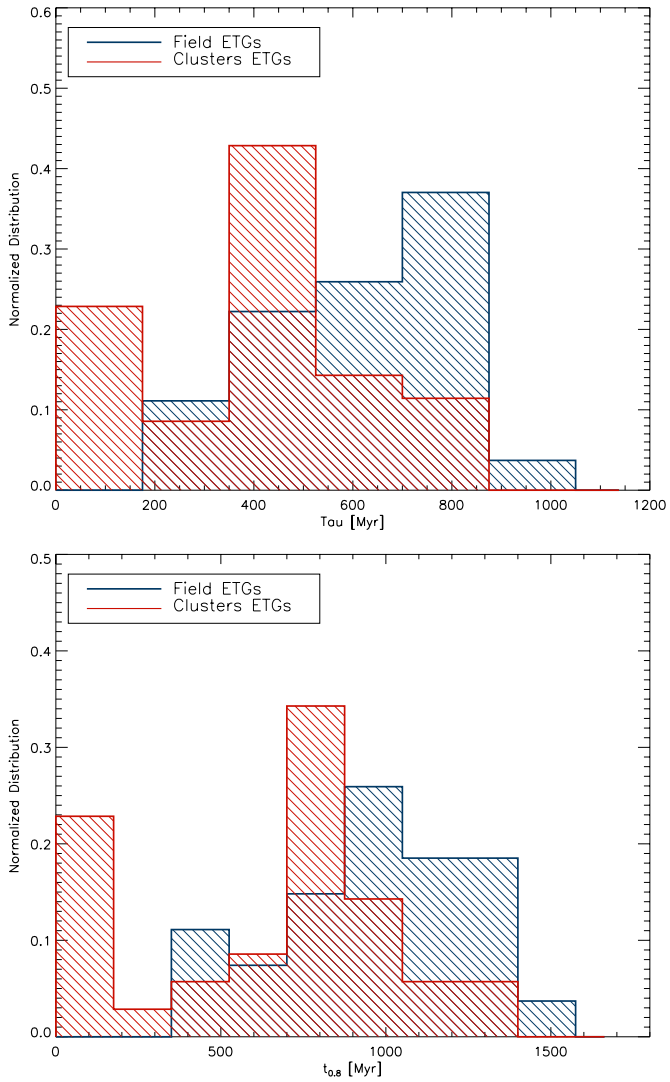

Figure 6. Top panel: histogram of the formation timescales, τ, of ETGs in both environments. Bottom panel: histogram of the times, $t_{0.8}$, needed for a given galaxy to form 80% of the stars it would have at $z = 0$, for both environments. Uncertainties in the determination of τ and $t_{0.8}$ are ∼0.2 and ∼0.4 Gyr, respectively.

(A color version of this figure is available in the online journal.)

given mass. In fact, the Mann–Whitney *U*-test confirms that the distributions are very likely to be different (median probability of 0.07%). The K-S statistic also yields an associated probability that the two distributions of τs are drawn from the same distribution of just 0.8%.

If galaxies continue to form stars following the exponential decay of Equation (1), we can derive the time $t_{0.8}$ needed to form 80% of the stars they would have at $z = 0$. As shown in the top right panel of Figure 5 and the bottom panel of Figure 6, we find that ∼1 Gyr after the onset of SF 75% of cluster ETGs have already assembled most of their final mass. By the same time, less than 35% of field ETGs have.

The bottom left panel of Figure 5 shows the relative distributions of the inferred initial SFR, SFR_0, as a function of stellar mass. More than 30% of cluster galaxies have higher SFR_0 and smaller τs than any other field contemporaries, indicating that they have experienced a much more intense SF at early times than field galaxies. As a result, at the time of observation, cluster ETG-specific SFRs, defined as the SFR divided by the galaxy stellar mass, SSFR, are lower than those of the field ones (bottom right panel of Figure 5). Indeed the Mann–Whitney *U*-test confirms that the distributions of SSFR are likely to be different (median probability of 1.3%). The K-S statistic yields an associated probability of 0.5% that the two distributions of τs are drawn from the same parent distribution.

As summarized by the histograms in Figure 6, the distributions of τ and $t_{0.8}$ in clusters and in the field are found to be very different. These results clearly indicate a dependence of ETGs' SFHs on the environment, in agreement with previous studies based on a comparison of a single cluster to the field (Gobat et al. 2008; Rettura et al. 2010; Menci et al. 2008).

As discussed in Rettura et al. (2010), we recall that our field sample is more deficient in lower mass objects than the cluster sample because of a less extensive follow-up of spectroscopic targets in the field as compared to that in the cluster.

However, even if the field sample were corrected for completeness, this would likely result in a larger fraction of field ETGs at low mass, which are the ones that we find with longer τs and $t_{0.8}$s, higher SSFRs and lower SFR_0s. Hence, a correction would actually amplify the difference between the typical mass assembly timescales of the two samples, and so not affect our conclusions.

5. CONCLUSIONS

We have studied the environmental dependence of ETG stellar population properties at $z \sim 1.3$ based on high-quality, multi-wavelength photometry available in 8–10 passbands from *U* to [4.5 μm]: sampling the entire relevant domain of emission of the different stellar populations, from rest-frame far-ultraviolet to the infrared.

We have similarly analyzed mass-selected samples of ETGs belonging to the cores of three massive clusters (RXJ0849+4452 at $z = 1.261$, RXJ0848+4453 at $z = 1.273$, and RDCS1252.9−2927 at $z = 1.237$) and compared their stellar population properties with those measured in a similarly selected sample of field contemporaries drawn from the GOODS-South survey.

We have derived stellar masses, (SF weighted) ages, and SFHs, parameterized as timescales, τ, from exponentially declining CSP model templates built with BC03 models for samples of massive ($M > 5 \times 10^{10}\ M_{\odot}$), passive (no-emission line in their spectra) ETGs at $z \simeq 1.3$. Apart from a lower level of spectroscopic completeness for the least massive field galaxies, that we find not to affect our conclusions, our sample has the advantage of being photometrically complete at our mass limit and having galaxy types (passive or star-forming members) assigned spectroscopically.

This work extends the analyses performed on a single cluster by Rettura et al. (2010) and Gobat et al. (2008) to two more clusters at $z \sim 1.3$, doubling the size of the cluster ETG sample.

Hence, on the basis of the new data we are able to affirm that

1. We find no significant difference in the derived stellar population properties of $z \sim 1.3$ ETGs belonging to different X-ray luminous clusters (RXJ0849+4452, RXJ0848+4453, and RDCS1252.9−2927).

Moreover, the comparative statistical analysis performed in this work on the extended data set corroborates the results obtained in our previous study (Rettura et al. 2010), which we summarize as follows:

1. Field ETGs are distributed around the cluster ETG red sequence, although they seem to show a larger scatter,

especially at lower masses. We will need more statistics and better estimates of uncertainties to draw more stringent conclusions, since the cluster and field overall scatters could still be consistent within the uncertainties. However, we recall that the small scatter in cluster environments remains a challenge for semi-analytical galaxy evolution models (Menci et al. 2008).

2. We find no significant delay in the (SF weighted) ages of massive ETGs observed in all clusters and in the field at $z \simeq 1.3$.
   The age of ETGs increases with galaxy mass in all environments, which is in agreement with the *downsizing* scenario. The site of active SF must have shifted from the most massive to the less massive galaxies as a function of the cosmic time. The formation epochs of ETGs only depend on their masses and not on the environment they live in. This result is in remarkably good agreement with those obtained from the evolution of the M/L (e.g., van Dokkum & van der Marel 2007 and di Serego Alighieri et al. 2006).
3. However, the data show that cluster and field SFHs are significantly different. Field ETG best-fit models span a different range of timescales than their cluster contemporaries, which are formed with the shortest τ at any given mass. This result is quantitatively consistent with the predictions of current galaxy formation models based on the latest rendition of semi-analytic models (Menci et al. 2008).
4. We find that 1 Gyr after the onset of SF 75% of cluster ETGs have already assembled 80% (or more) of their final mass, while, by the same time, less than 35% of field ETGs have.
5. Accordingly, cluster ETG-specific SFRs at the time of observation are found to be smaller than those of the field ones, implying that the last episode of SF must have happened more recently in the field than in the cluster.

While cluster and field galaxies observed at $z \simeq 1.3$ form at a similar epoch in a statistical sense, a high-density environment appear to be able to trigger a much more rapid and homogenous mass assembly event for the ETGs, limiting the range of possible SF processes. In fact, more than 30% of cluster galaxies are found with higher initial SFR_0 and smaller τs than any other field contemporaries, indicating they have experienced much more intense SF at early times than field galaxies. In low density environments, this effect must rapidly fade as ETGs display a much broader range of possible SFHs.

A.R. is grateful to Gabriella de Lucia, Raphael Gobat, Roderik Overzier, Maurilio Pannella, Veronica Strazzullo, and Loredana Vetere for useful discussions.

ACS was developed under NASA contract NAS 5-32865. This research has been supported by the NASA *HST* grant GO-10574.01-A, and *Spitzer* program 20694. The Space Telescope Science Institute is operated by AURA Inc., under NASA contract NAS5-26555. Some of the data presented herein were obtained at the W. M. Keck Observatory, which is operated as a scientific partnership among the California Institute of Technology, the University of California and the National Aeronautics and Space Administration. The Observatory was made possible by the generous financial support of the W. M. Keck Foundation. The authors wish to recognize and acknowledge the very significant cultural role and reverence that the summit of Mauna Kea has always had within the indigenous Hawaiian community. They are most fortunate to have the opportunity to conduct observations from this mountain. Some data were based on observations obtained at the Gemini Observatory, which is operated by the AURA, Inc., under a cooperative agreement with the NSF on behalf of the Gemini partnership: the National Science Foundation (United States), the Science and Technology Facilities Council (UK), the National Research Council (Canada), CONICYT (Chile), the Australian Research Council (Australia), Ministerio da Ciencia e Tecnologia (Brazil), and Ministerio de Ciencia, Tecnologia e Innovacion Productiva (Argentina), Gemini Science Program ID: GN-2006A-Q-78. R.D. acknowledges the support provided by the BASAL Center for Astrophysics and Associated Technologies and by FONDECYT grant N. 1100540.

REFERENCES

Adelberger, K. L., Steidel, C. C., Pettini, M., Shapley, A. E., Reddy, N. A., & Erb, D. K. 2005, ApJ, 619, 697
Balestra, I., et al. 2010, A&A, 512, A12
Balogh, M. L., et al. 2002, ApJ, 566, 123
Bell, E. F., McIntosh, D. H., Katz, N., & Weinberg, M. D. 2003, ApJS, 149, 289
Bernardi, M., Renzini, A., da Costa, L. N., Wegner, G., Alonso, M. V., Pellegrini, P. S., Rité, C., & Willmer, C. N. A. 1998, ApJ, 508, L143
Blakeslee, J. P., et al. 2003, ApJ, 596, L143
Blakeslee, J. P., et al. 2006, ApJ, 644, 30
Bower, R. G., Benson, A. J., Malbon, R., Helly, J. C., Frenk, C. S., Baugh, C. M., Cole, S., & Lacey, C. G. 2006, MNRAS, 370, 645
Bruzual, G., & Charlot, S. 2003, MNRAS, 344, 1000
Burstein, D., Bertola, F., Buson, L. M., Faber, S. M., & Lauer, T. R. 1988, ApJ, 328, 440
Cardelli, J. A., Clayton, G. C., & Mathis, J. S. 1989, ApJ, 345, 245
Cimatti, A., et al. 2002, A&A, 391, L1
Cimatti, A., et al. 2004, Nature, 430, 184
Clemens, M. S., Bressan, A., Nikolic, B., Alexander, P., Annibali, F., & Rampazzo, R. 2006, MNRAS, 370, 702
Collins, C. A., et al. 2009, Nature, 458, 603
Cowie, L. L., Songaila, A., Hu, E. M., & Cohen, J. G. 1996, AJ, 112, 839
De Lucia, G., Springel, V., White, S. D. M., Croton, D., & Kauffmann, G. 2006, MNRAS, 366, 499
Demarco, R., et al. 2007, ApJ, 663, 164
De Propris, R., Stanford, S. A., Eisenhardt, P. R., Holden, B. P., & Rosati, P. 2007, AJ, 133, 2209
Diaferio, A., Kauffmann, G., Balogh, M. L., White, S. D. M., Schade, D., & Ellingson, E. 2001, MNRAS, 323, 999
di Serego Alighieri, S., Lanzoni, B., & Jørgensen, I. 2006, ApJ, 652, L145
di Serego Alighieri, S., et al. 2005, A&A, 442, 125
Dressler, A., et al. 1997, ApJ, 490, 577
Eisenhardt, P. R. M., et al. 2008, ApJ, 684, 905
Fontana, A., et al. 2004, A&A, 424, 23
Giavalisco, M., et al. 2004, ApJ, 600, L93
Gobat, R., Rosati, P., Strazzullo, V., Rettura, A., Demarco, R., & Nonino, M. 2008, A&A, 488, 853
Gunn, J. E., & Gott, J. R. I. 1972, ApJ, 176, 1
Hilton, M., et al. 2009, ApJ, 697, 436
Holden, B. P., et al. 2005, ApJ, 620, L83
Jørgensen, I., Chiboucas, K., Flint, K., Bergmann, M., Barr, J., & Davies, R. 2006, ApJ, 639, L9
Juneau, S., et al. 2005, ApJ, 619, L135
Kochanek, C. S., et al. 2000, ApJ, 543, 131
Kodama, T., & Bower, R. G. 2001, MNRAS, 321, 18
Kodama, T., Tanaka, I., Kajisawa, M., Kurk, J., Venemans, B., De Breuck, C., Vernet, J., & Lidman, C. 2007, MNRAS, 377, 1717
Lidman, C., Rosati, P., Demarco, R., Nonino, M., Mainieri, V., Stanford, S. A., & Toft, S. 2004, A&A, 416, 829
Lidman, C., et al. 2008, A&A, 489, 981
Maraston, C. 1998, MNRAS, 300, 872
Maraston, C. 2005, MNRAS, 362, 799
Mei, S., et al. 2006a, ApJ, 644, 759
Mei, S., et al. 2006b, ApJ, 639, 81
Mei, S., et al. 2009, ApJ, 690, 42
Mei, S., et al. 2011, submitted
Menci, N., Rosati, P., Gobat, R., Strazzullo, V., Rettura, A., Mei, S., & Demarco, R. 2008, ApJ, 685, 863
Miley, G., & De Breuck, C. 2008, A&AR, 15, 67

Moore, B., Ghigna, S., Governato, F., Lake, G., Quinn, T., Stadel, J., & Tozzi, P. 1999, ApJ, 524, L19
Moore, B., Katz, N., Lake, G., Dressler, A., & Oemler, A. 1996, Nature, 379, 613
Moore, B., Lake, G., & Katz, N. 1998, ApJ, 495, 139
Nakata, F., et al. 2005, MNRAS, 357, 1357
Nonino, M., et al. 2009, ApJS, 183, 244
Overzier, R. A., et al. 2009, ApJ, 704, 548
Pannella, M., et al. 2009, ApJ, 701, 787
Papovich, C., et al. 2010, ApJ, 716, 1503
Postman, M., et al. 2005, ApJ, 623, 721
Press, W. H., Teukolsky, S. A., Vetterling, W. T., & Flannery, B. P. 1992, Numerical Recipes in FORTRAN (2nd ed.; Cambridge: Cambridge Univ. Press)
Raichoor, A., et al. 2011, arXiv:1103.0259R
Renzini, A. 2006, ARA&A, 44, 141
Rettura, A., et al. 2006, A&A, 458, 717
Rettura, A., et al. 2010, ApJ, 709, 512
Retzlaff, J., et al. & GOODS Team. 2010, A&A, 511, A50
Rosati, P., Stanford, S. A., Eisenhardt, P. R., Elston, R., Spinrad, H., Stern, D., & Dey, A. 1999, AJ, 118, 76
Rosati, P., et al. 2009, A&A, 508, 583
Salpeter, E. E. 1955, ApJ, 121, 161
Sánchez-Blázquez, P., Gorgas, J., Cardiel, N., & González, J. J. 2006, A&A, 457, 809
Saracco, P., et al. 2004, A&A, 420, 125
Spergel, D. N., et al. 2003, ApJS, 148, 175
Stanford, S. A., Elston, R., Eisenhardt, P. R., Spinrad, H., Stern, D., & Dey, A. 1997, AJ, 114, 2232
Stanford, S. A., Holden, B., Rosati, P., Tozzi, P., Borgani, S., Eisenhardt, P. R., & Spinrad, H. 2001, ApJ, 552, 504
Steidel, C. C., Adelberger, K. L., Shapley, A. E., Erb, D. K., Reddy, N. A., & Pettini, M. 2005, ApJ, 626, 44
Strazzullo, V., et al. 2006, A&A, 450, 909
Strazzullo, V., et al. 2010, A&A, 524, A17
Tanaka, M., De Breuck, C., Venemans, B., & Kurk, J. 2010a, A&A, 518, A18
Tanaka, M., Finoguenov, A., & Ueda, Y. 2010b, ApJ, 716, L152
Tantalo, R., Chiosi, C., Bressan, A., & Fagotto, F. 1996, A&A, 311, 361
Thomas, D., Maraston, C., Bender, R., & Mendes de Oliveira, C. 2005, ApJ, 621, 673
Toft, S., Mainieri, V., Rosati, P., Lidman, C., Demarco, R., Nonino, M., & Stanford, S. A. 2004, A&A, 422, 29
Treu, T., Stiavelli, M., Bertin, G., Casertano, S., & Møller, P. 2001, MNRAS, 326, 237
Treu, T., Stiavelli, M., Casertano, S., Møller, P., & Bertin, G. 1999, MNRAS, 308, 1037
Treu, T., et al. 2005, ApJ, 633, 174
van der Wel, A., Franx, M., van Dokkum, P. G., Rix, H.-W., Illingworth, G. D., & Rosati, P. 2005, ApJ, 631, 145
van Dokkum, P. G., & Franx, M. 1996, MNRAS, 281, 985
van Dokkum, P. G., & Franx, M. 2001, ApJ, 553, 90
van Dokkum, P. G., & Stanford, S. A. 2003, ApJ, 585, 78
van Dokkum, P. G., & van der Marel, R. P. 2007, ApJ, 655, 30
Vanzella, E., et al. 2005, A&A, 434, 53
Vanzella, E., et al. 2006, A&A, 454, 423
Vanzella, E., et al. 2008, A&A, 478, 83
Worthey, G. 1994, ApJS, 95, 107
Yi, S., Demarque, P., & Oemler, A. J. 1997, ApJ, 486, 201
Yi, S., Lee, Y.-W., Woo, J.-H., Park, J.-H., Demarque, P., & Oemler, A. J. 1999, ApJ, 513, 128